Pure Appl. Chem., Vol. 84, No. 4, pp. 979–989, 2012.
http://dx.doi.org/10.1351/PAC-CON-11-10-14

A programmable single-component diode based on an ambipolar organic field-effect transistor (OFET)*

Tadashi Sugawara[1,‡], Takuro Itoh[1], Kentaro Suzuki[1], Hiroyuki Higuchi[2], and Michio M. Matsushita[3]

[1]Department of Basic Science, Graduate School of Arts and Sciences, The University of Tokyo, 3-8-1 Komaba, Meguro, Tokyo 153-8902, Japan; [2]Department of Chemistry, Faculty of Science, Toyama University, 3190 Gofuku, Toyama 930-8555, Japan; [3]Department of Chemistry, Nagoya University, Chikusa-ku, Nagoya 464-8602, Japan

Abstract: An ambipolar field-effect transistor (FET) based on tetracyanoquarterthienoquinoid (TCT_4Q) was constructed. When a set of source, drain, and gate voltages were applied to a thin film of TCT_4Q at temperatures lower than 150 K, both positive and negative carriers were trapped and frozen even after removal of the gate voltage. The frozen carriers worked as a floating gate with the gradient by creating a PN(NP) junction through the injection of oppositely charged "mobile" carriers. The device exhibited a distinct rectifying effect when an alternating current ($50 < f < 500$ mHz) was applied through the source and drain electrodes. Moreover, the function of the molecular device is programmable and erasable.

Keywords: materials chemistry; molecular electronics; X-ray structure.

INTRODUCTION

π-Conjugated molecules that can be aromatized through redox processes are effective for forming mixed valence states which are necessary for creating molecular conductors. For example, tetrathiafulvalene (TTF), which is a hetero-analogue of heptafulvalene, has a 6π-electron configuration upon single-electron oxidation of one of the dithiole rings. This singly oxidized species is important because the conductivity of such a π-conjugated molecular solid is interpreted in terms of intermolecular migration of aromaticity [1]. On the other hand, tetracyanoquinodimethane (TCNQ), a good acceptor with a quinoid structure, is an indispensable building block of conductive charge-transfer complexes. Single-electron reduction of TCNQ creates an anion radical having a benzenoid electronic structure by localizing an ionic charge and an unpaired electron at individual methylene carbons of the dicyanomethylene groups [2,3]. The property of a molecular solid or self-assembled structure of these redox-active π-conjugated molecules, however, must be switched by an external electric field [4].

A bottom gate-type field-effect transistor (FET), which consists of a pair of source and drain electrodes fabricated on a dielectric layer (SiO_2) atop a gate electrode made of *n*-doped silicon, is a powerful tool to create charged species. Holes or electrons are injected into a neutral crystal placed on the substrate by applying a gate voltage. The FET is able to utilize the unique characteristics of the organic molecules because: (1) it does not require a large single crystal for electric measurements, (2) it is not

Pure Appl. Chem.* **84, 861–1112 (2012). A collection of invited papers based on presentations at the 14th International Symposium on Novel Aromatic Compounds (ISNA-14), Eugene, OR, USA, 24–29 July 2011.
‡Corresponding author

necessary to form ion radical salts or charge transfer complexes to measure transport properties, and (3) it can create charge carriers in a neutral crystal by electron or hole injection from the electrodes. Among redox-active π-conjugated molecules, a special group of molecules, called "ambipolar molecules," can be both oxidized and reduced under moderate oxidation and reduction potentials. Highly conjugated polyaromatic hydrocarbons usually show ambipolar owing to the relatively small highest occupied molecular orbital–lowest unoccupied molecular orbital (HOMO–LUMO) gap. Thus far, most ambipolar organic field-effect transistors (OFETs), however, have been based on co-evaporated films, copolymers, or bilayer structures composed of weak donors and acceptors [5–7]. Ambipolar FETs based on a single small molecule (e.g., pentacene) have been constructed, but the Fermi levels of the source and drain electrodes were forced to match those of the conduction and valence bands of the pentacene, respectively [8]. Only a few unicomponent ambipolar FET devices have been reported [9–12]. Because ambipolar molecules can carry both holes and electrons, the following question may arise: Is it possible to construct a single-component molecule-based diode utilizing such ambipolar compounds?

To begin to address this possibility, the tetracyanoquinoid family [13] is hopeful. They have acceptor character derived from tetracyanoquinoid structure, and the donor character is enhanced as the number of thienoquinoid units (n) is increased. Cyclic voltammograms of a series of oligothienoquinoids show that, while only the reduction wave is obtained from tetracyanodithienoquinoid (n = 2), both reduction and oxidation waves can be recorded for tetracyanoterthienoquinoid (n = 3). However, the oxidation potential of the latter was higher than 1 V. In the case of tetracyanoquarterthienoquinoid (TCT_4Q) (n = 4, Fig. 1), the potential difference becomes smaller than 1 V, suggesting that TCT_4Q is an excellent ambipolar compound for molecule-based diodes [14]. TCT_4Q reduces to give a dianion by electrochemical two-electron reduction, as has been shown in UV spectral investigation [14]. TCT_4Q can also be electrochemically oxidized to give a cation radical [14]. These experimental results reveal that the charged species are reasonably stable because of the contribution of the benzenoid character.

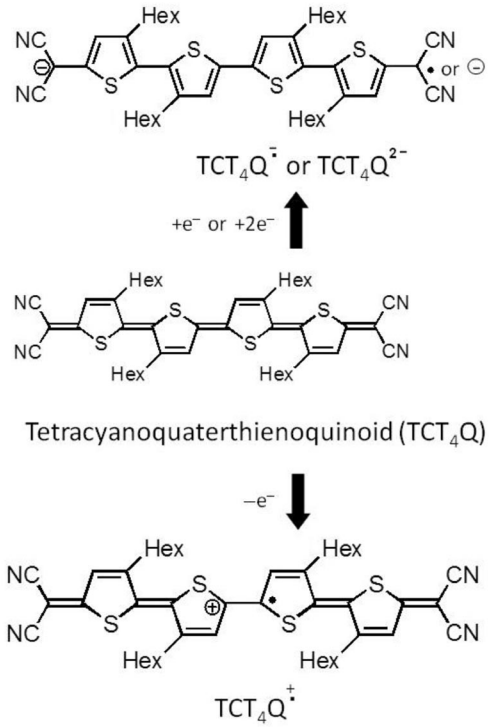

Fig. 1 Resonance structures of neutral, anion radical (dianion), and cation radical of TCT_4Q.

In a silicon-based diode, connection of *p*-doped and *n*-doped silicon leads to a PN junction. If voltage is applied in the forward direction, holes in a valence band and electrons in a conduction band flow between the electrodes in opposing directions and recombine each other. The current therefore runs smoothly from one end to the other. However, if the electrode voltages are switched, holes and electrons are attracted to each electrode, respectively. Under these circumstances, the deficient zone of carriers in the middle of the electrodes expands. As a result, current cannot flow under a reversed bias. If TCT_4Q is able to carry both electrons and holes by applying positive and negative gate voltages, respectively (Figs. 2a,b), an FET device constructed by TCT_4Q may work as a diode exhibiting a rectifying effect. However, when the gate voltage of the FET device is removed, the carriers disappear, leaving no *n*- and *p*-doped domains (Fig. 2c). To achieve a molecule-based diode, spatially separated *p*- and *n*-doped regions must be in place to serve as a PN junction (Fig. 2d).

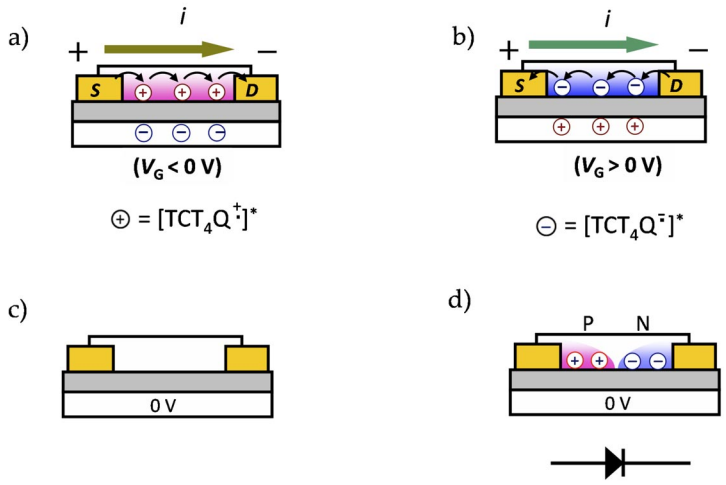

Fig. 2 (a) Charge transport by positive carriers from source to drain electrodes under the negative gate voltage. Current flows from source to drain electrodes. [$TCT_4Q^{+\cdot}$]* represents the cation radical with a neutral molecular structure. (b) Charge transport by negative carriers from drain to source electrodes. [$TCT_4Q^{-\cdot}$]* represents the anion radical with a neutral molecular structure. (c) Carriers are extinguished when the gate voltage is removed ($V_G = 0$) at ambient temperature (see text). (d) A molecule-base diode with a PN junction in an organic thin layer (the gate voltage is removed). When alternating current is applied, the output current is rectified.

Herein, the conversion of a TCT_4Q-based ambipolar FET device into a single-component diode is described. Two additional steps were required after the FET device was fabricated. First, positively and negatively charged carriers were injected into the gap between the electrodes. These charged carriers were easily trapped through the formation of stable charged cation or anion radicals of TCT_4Q (Fig. 1). Second, the "trapped carriers" were frozen at low temperatures to prevent recombination even after the removal of the gate voltage. The "trapped carriers" then served as a "floating gate", which induced a PN junction through the injection of mobile carriers with opposite charges (Fig. 2d). Finally, the device exhibited a rectifying function when alternating current was applied between source and drain electrodes.

EXPERIMENTAL

Materials

TCT_4Q was synthesized as reported elsewhere [13], and stored in powder form in a refrigerator. It was purified using a short column of silica gel (0.063–0.200 mm, Merck) and eluted with chloroform. The purified powders were recrystallized from dichloromethane and *n*-hexane (3:1 *v*/*v*) before use. Organic solvents (special grade) were purchased from Kanto Chemical Co., Inc.

Preparation of FET device

In a glove box filled with nitrogen gas, a thin film of TCT_4Q was prepared by solution casting. A chloroform solution of TCT_4Q (ca. 2 mM) was dropped onto the substrate using a glass capillary (i.d. = 0.3 mm) and dried gently. Interdigitated Au electrodes having a total length of 1 m and folded in a square of 2 × 2 mm^2 with a gap of 2 μm (Tonic Co., Ltd.) were formed on SiO_2 (thickness = 300 nm) atop a gate electrode made of heavily *n*-doped silicon (thickness of ca. 1 mm). The fabricated sample was inspected with a digital microscope (Keyence VHX-1000).

Silylation of the cleaned substrate surface was carried out using octadecyltrichlorosilane as a silylating reagent as follows [15]. The interdigitated electrodes were placed in Cica Clean LX-3 (Kanto Chemical Co., Inc.) overnight. The electrodes were then rinsed with deionized water and dried at 110 °C for 20 min under a flow of nitrogen. The rinsed and dried electrodes were then placed in a solution of octadecyltrichlorosilane (5 mM) in toluene for 18 h at 25 °C under a nitrogen atmosphere. The silylated substrate was finally rinsed with dry toluene.

X-ray diffraction measurement

Although TCT_4Q usually affords fine powders, recrystallization from dichloromethane/*n*-hexane (3:1 *v*/*v*) using a cautiously purified sample as described in the MATERIALS gave very thin plates in a polycrystalline state. A thin platelet crystal (0.300 × 0.120 × 0.005 mm) was peeled by a pair of tweezers and was mounted on a loop of the diffractometer. The analyzed crystal was the best among several of them. All measurements were made on a R-AXIS RAPID diffractometer (Rigaku) using filtered Cu-Kα radiation. The crystal-to-detector distance was 127.40 mm. Cell constants and an orientation matrix for data collection corresponded to a primitive triclinic cell with dimensions: a = 7.9342(6), b = 9.8038(6), c = 14.781(3) Å, α = 101.88(2), β = 99.19(2), γ = 99.36(2)º, V = 1087.7(3) $Å^3$. For Z = 1 and F.W. = 793.22, the calculated density is 1.211 g/cm^3. Based on a statistical analysis of the intensity distribution, and a successful solution and refinement of the structure, the space group was determined to be P-1 (#2).

The data were collected at 153 ± 1 K to a maximum 2θ value of 136.5º. All data were measured using ω scans. Of the measured 12 269 reflections, 3881 were unique (R_{int} = 0.1302). The linear absorption coefficient, μ, for Cu-Kα radiation is 22.739 cm^{-1}. An empirical absorption correction was applied, which resulted in transmission factors ranging from 0.530 to 0.989. The structure was elucidated by direct methods and expanded using Fourier techniques. The non-hydrogen atoms were refined anisotropically. Hydrogen atoms were refined using the riding model. The final cycle of full-matrix least-squares refinement on F^2 was based on 3877 observed reflections and 245 variable parameters and converged with unweighted and weighted agreement factors of:

$$R_1 = \Sigma \, ||F_o| - |F_c|| \, / \, \Sigma \, |F_o| = 0.1284$$

$$wR_2 = [\, \Sigma \, (w(F_o^2 - F_c^2)^2) \, / \, \Sigma \, w(F_o^2)^2]^{1/2} = 0.3281$$

The standard deviation of an observation of unit weight was 1.08. Unit weights were used. The maximum and minimum peaks on the final difference Fourier map corresponded to 0.85 and

–0.39 $e^{-}/Å^3$, respectively. Neutral atom scattering factors were taken from Cromer and Waber [16]. Anomalous dispersion effects were included in Fcalc [17]. Values for $\Delta f'$ and $\Delta f''$ were those of Creagh and McAuley [18]. The values for the mass attenuation coefficients are those of Creagh and Hubbell [19]. All calculations were performed using the CrystalStructure crystallographic software package (Rigaku), except for refinement, which was performed using SHELXL-97.

Measurement of transfer characteristics at ambient temperature

Each electrode of the device was connected to a source meter (Advantest R6245) and the V_G–I_{SD} characteristics of the FET were measured at room temperature under nitrogen with V_{SD} = 5 V, and V_G swept from –20 V to +20 V in steps of 1 V/ 200 ms.

Measurement of I_{SD}–V_G at low temperature after field cooling

Temperature of the device was controlled by the cryostat of a SQUID instrument (Quantum Design MPMS). The FET device was attached to gold wire (25 μm) with gold paste (Tokuriki Chemical Research Co., Ltd.), soldered to copper pads at the top of a hand-made probe (overall length = 1400 mm, probe length = 130 mm, rod diameter = 3 mm, probe diameter = 6.5 mm), and was inserted into a sample holder of the cryostat.

Measurement of transfer characteristics under Various V_G

Various gate voltages [V_G(set)] were set to the FET device by a DC source (Keithley 2400) for 5 min at 300 K (V_G(set) = –30, –20, –10, 0, 10, 20, 30 V). The device was cooled to 100 K at a rate of 10 K/min while applying individual V_G(set). After cooling, V_G(set) was removed and the V_G–I_{SD} characteristics were measured by a source meter (Advantest R6245) with V_{SD} = 10 V, and V_G swept from –50 V to +50 V in steps of 1 V/200 ms

Formation of PN junction and its response toward AC

A gate voltage (V_G = 20 V) was applied by a DC source (Keithley 2400) and the source and drain voltages (V_S = 40, V_D = 0 V) by a DC source (Keithley 6487) at 300 K for 5 min. The device was cooled down to 100 K at a rate of 10 K/min while applying V_G and V_{SD}. After cooling, individual voltages (V_S, V_D, and V_G) were removed. Alternating triangular voltage ($V_{p–p}$ = 4 V, V_G = 0 V, f = 50 mHz) supplied by a function generator (NF 1920A) was amplified 10 times by a bipolar power supply (Takasago BPS120-5), and it was applied between source and drain electrodes. Currents were measured with an ammeter (Keithley 6487), and the voltage was measured using a multimeter (Keithley 2000).

RESULTS AND DISCUSSION

Physical properties and crystal structure of TCT_4Q

The ambipolar character of TCT_4Q is readily observed from MO calculations (B3LYP/6-31G*) of a series of oligothienoquinoids. Although the energy level of the LUMO remains almost the same, the energy level of the HOMO increases as the π-conjugation length is increased. As a result, the energy gap between the HOMO and LUMO decreases significantly (Fig. 3).

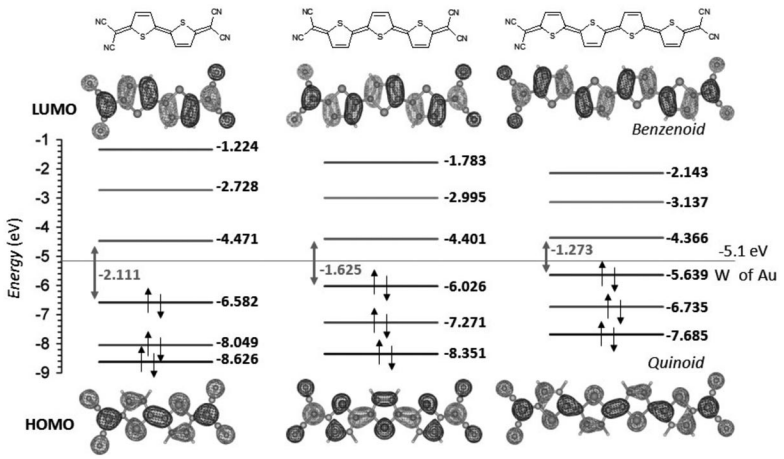

Fig. 3 Energy levels and shapes of frontier molecular orbitals of a series of thienoquinoid derivatives calculated by B3LYP/6-32G*.

The change of bond lengths and charge densities associated with the oxidation or reduction of TCT_4Q were compared with those found in the literature [14]. In performing a Mulliken net charge analysis, neutral TCT_4Q was found to be appreciably polarized, even in the ground state. The net charge density of dicyanomethylene group [$C(CN)_2$] is –0.32, the outer thiophene ring is +0.20, and the inner ring is +0.12. Whereas the shapes of the HOMOs are of a quinoid type, having bonding character in the olefinic double bonds, those of the LUMOs are of a benzenoid character, having bonding character in double bonds of a thiophene ring. Reduction of TCT_4Q makes the C1–C1' bond longer (Δd = 0.028 Å for anion radical; Δd = 0.050 Å for dianion) because the incoming electron occupies the LUMO. Oxidation of TCT_4Q also elongates the C1–C2 bond (Δd = 0.024 Å) because the bonding character is weakened by removal of an electron from the HOMO.

The crystal structure of TCT_4Q, determined by X-ray diffraction method, was shown in Fig. 4. Although the final *R* value was 13 % because the very thin platelet shape of the single crystal (thickness is 0.05 mm), the quality of the analyzed data is sufficiently good to discuss the molecular arrangement, π–π staking structure. These crystal structure data are indispensable to discuss the precise mechanism of the charge-transport property in the FET device. The crystal structures of some oligothienoquinoides have been reported, but the packing pattern of TCT_4Q is unique [20]. Viewed along the direction perpendicular to the molecular plane of quarterthienoquinoid, TCT_4Q forms a 1D array through the dipolar interaction between the dicyanomethylene groups with an intermolecular distance of 3.36 Å between the carbon and nitrogen atoms (Fig. 4a). The hexyl groups are all-trans and extend between 1D arrays of the oligothieno units. When viewed along the *c*-axis, halves of two adjacent quarterthienyl groups stack upon each other through the electrostatic interaction between the negatively charged dicyanomethylene group and the positively charged oligothieno unit (Fig. 4b). Thus, one TCT_4Q is layered between four TCT_4Q molecules. The thin-plate crystal consisted of large {0 0 1}, narrow, and long {1 0 0}, and narrow and short {1 –1 0} planes. If {0 0 1} is defined as the plane of the substrate, the 2D layer of oligothieno units (Fig. 4b) is parallel to the substrate. The thin narrow and long plane, which corresponds to the conductive direction, can therefore act as a bridge between the source and drain electrodes. This alignment could produce the observed FET characteristics.

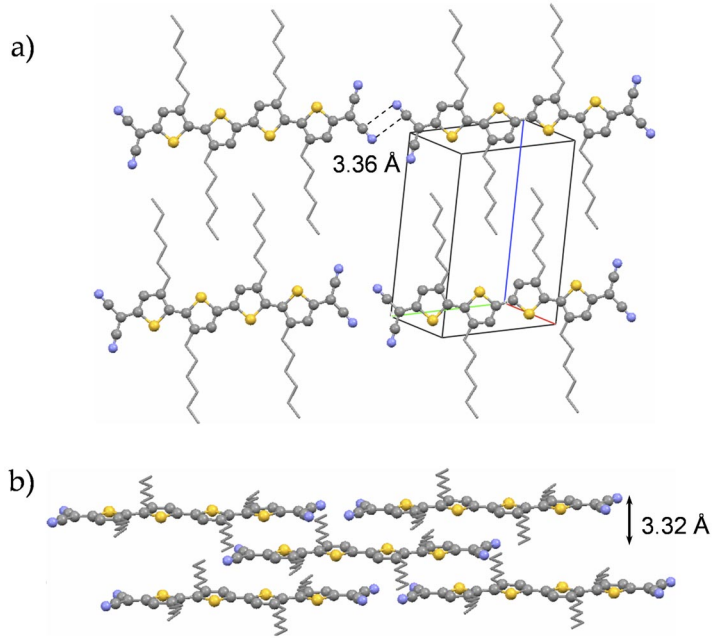

Fig. 4 Crystal structure of TCT_4Q. (a) Viewed along the perpendicular direction to the molecular plane of quarterthienoquinoid. (b) Viewed along the *c*-axis. The stacking distance of TCT_4Q is 3.22 Å.

Construction and characteristics of OFET made of TCT_4Q

An FET was constructed by solution casting TCT_4Q on interdigitated electrodes with a gap of 2 μm. Figures 5a,b show microscopic images of the single crystal of TCT_4Q and crystals on the interdigitated electrodes. The alignment of crystals attached to the interdigitated electrodes on the SiO_2 substrate is such that the flat surface of the crystal, corresponding to {0 0 1}, is mounted on top of the electrodes. As discussed above, stacking of the oligothieno groups, corresponding to the conduction path, is located parallel to the substrate.

Measurement of the transfer characteristics resulted in electron and hole mobility values of 1.1×10^{-4} and 6.0×10^{-4} cm^2/V s, respectively. Figure 5c shows the distinct V-shaped curve of the transfer characteristic. The I_{SD} current increases as the absolute value of the gate voltage V_G increases in both the positive and negative directions along the horizontal axis, reflecting the ambipolar character of the TCT_4Q. This characteristic has, in fact, been reported for tetracyanoterthienoquinoid with the different length and substitution pattern of alkyl chains [9]. However, the behavior is more distinct in TCT_4Q. Another feature of the TCT_4Q-based FET is a temporal decay of I_{SD} at a fixed V_G (the half-life of TCT_4Q is shorter than 1 s at 300 K). In the case of an FET based on pentacene, the reversible transfer characteristic was recorded in reference to the scanning along the V_G axis, whereas the TCT_4Q device showed distinct irreversible behavior. These results indicate that the temporal decay of I_{SD} of TCT_4Q is appreciably faster than that of pentacene [21].

The reason for the rapid decay of I_{SD} may be derived from the stability of the charged species. If a positive gate voltage (e.g., V_G = 10 V) is applied, the negative carrier, which corresponds to the $[TCT_4Q^{-\cdot}]^*$ that captures an electron but maintains the molecular geometry of the neutral species, is injected from the negative electrode (Fig. 2a). The negative charge is then conveyed from molecule to molecule through a relay mechanism, giving rise to I_{SD}. However, a negative carrier that fails to deliver the charge to the adjacent molecule is converted to a "trapped carrier" $[TCT_4Q^{-\cdot}]$, which is an anion

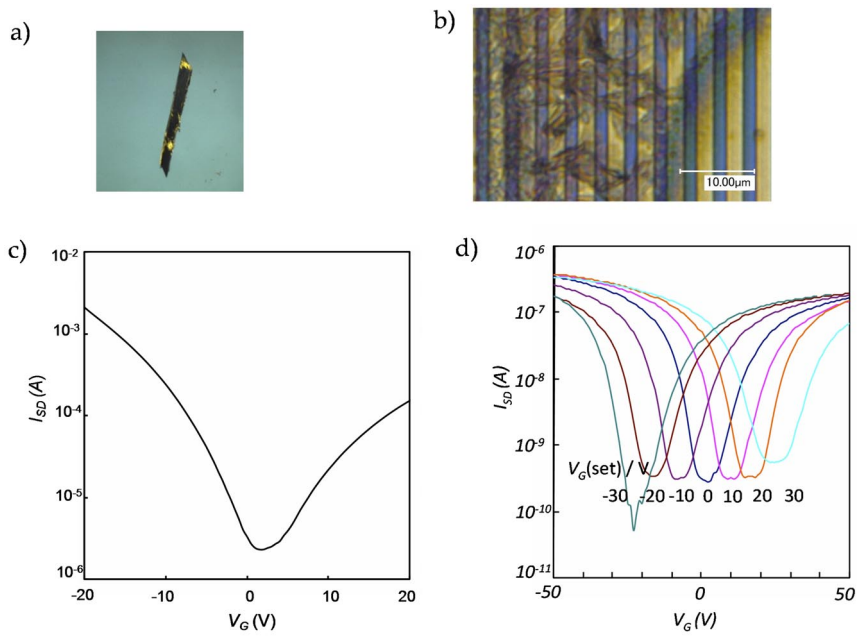

Fig. 5 (a) Microscopic images of a single crystal. (b) Crystals on interdigitated electrodes with a gap of 2 mm. (c) Ambipolar transfer characteristic of FET based on TCT_4Q with source–drain voltage of 5 V (V_{SD} = 5 V); gate voltage (V_G) was scanned in a range –20 V to 20 V with a step of 1 V/200 ms (total recording time was 8 s) at ambient temperature. (d) Ambipolar characteristics of FET based on TCT_4Q with a series of gate voltages [V_G(set) = 30, 20, 0 , –10, –20, –30 V] at 100 K.

radical with the stabilized geometry and is solvated by surrounding molecules. I_{SD} becomes null when all the carriers are trapped.

The change of the transfer characteristics of the device, measured after freezing the carrier at low temperature, is demonstrated as a shift of the minimum of the *I–V* curve from 0 to 10 V. The negative charge of the "trapped carriers" is balanced by the applied gate voltage (V_G = 10 V), and no excess mobile carriers exist at this gate voltage. In other words, the FET remembers the originally set gate voltage [V_G(set)] as the minimum in the *I–V* curve. In this case, a "trapped carrier" remains even after removal of the gate voltage because the thermal energy is not enough to re-mobilize a trapped carrier. Such a trapped carrier is called a "frozen carrier". A series of gate voltages were memorized at low temperature, shown in Fig. 5d, using the following procedure: First, a gate voltage [V_G(set)] is applied at ambient temperature, and then the organic film is frozen at 100 K, keeping the gate voltage applied. Second, the gate voltage is removed at 100 K, and the FET characteristics are measured. From the above procedure, it is clear that the ambipolar FET memorizes any set voltages, at least in the range from –30 V to 30 V. These characteristics of the TCT_4Q-FET were not changed when the substrate (SiO_2) was silylated by octadecyltrichlorosilane. This result suggests that the memory effect is derived from the trapped carrier inside the TCT_4Q crystal, although the possibility of the trapping by defects or impurities on the silicone surface cannot be completely excluded.

Creation of PN(NP) junction by a set of voltages (V_S, V_D, and V_G)

From the above experimental results, it is reasonable to infer that if V_S, V_D (e.g., 40 and 0 V, respectively), and V_G (e.g., 20 V) are applied at ambient temperature, ambipolar molecules (TCT_4Q)

near the source electrode would be subjected to the negative voltage while those near the drain electrode would be subjected to the positive voltage owing to a gradient of the "effective" gate voltage in the range of –20 and +20 V (Figs. 6a,d). Since these carriers are trapped at ambient temperature (Figs. 6b,e) and are frozen at temperatures lower than 150 K (Figs. 6b,e), the "trapped carriers" may work as a floating gate with the gradient after V_G is removed (Fig. 6c). Then the oppositely charged carriers will be injected from electrodes, responding to the gradient caused by the floating gate. As a result, an NP junction (from left to right) will be created in the device (Figs. 6c,f,g).

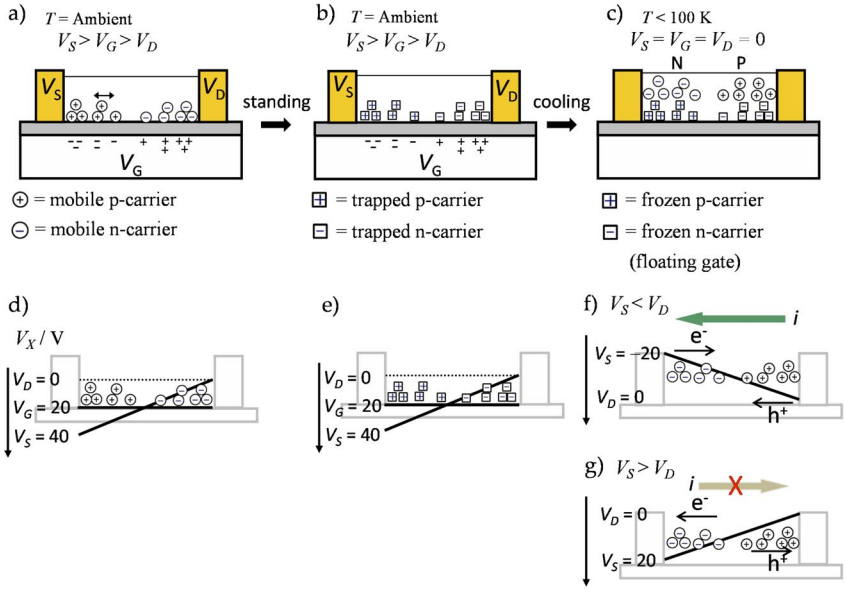

Fig. 6 (a) Distribution of positive and negative "mobile" carriers injected from electrodes under application of the gradient effective gate voltage ($V_S > V_G > V_D$) at ambient temperature. ⊕ denotes a positive mobile carrier, ⊖ denotes a negative mobile carrier. (b) Distribution of "trapped" carriers under gradient gate voltage ($V_S > V_G > V_D$) at ambient temperature, ⊞ denotes a positive trapped carrier, ⊟ denotes a negative trapped carrier. (c) Reinjection of carriers was induced by the floating gate derived from "frozen" carriers after removal of gate voltage at low temperature, ⊞ denotes a positive frozen carrier, ⊟ denotes a negative frozen carrier. (d) Gradient voltage applied in the case (a) with V_S = 40 V, V_G = 20 V, V_D = 0. (e) Gradient voltage applied in the case (b) with V_S = 40 V, V_G = 20 V, V_D = 0. (f) Forward bias operation ($V_S < V_D$) in the case of (c). (g) Reverse bias operation ($V_S > V_D$) in the case of (c). No current flows through the organic thin film.

In fact, when an alternating current (alternating triangular voltage with V_{p-p} = 40 V, 50 mHz < f < 500 mHz) was applied through the SD electrodes with V_S = –20, V_D = 0 V, and V_G = 0 V to the thin film which had been "trained" according to the above procedure (Fig. 6f), current was detected only when the negative voltage was applied to the device, therefore exhibiting the rectifying function (Fig. 7a). The reproducibility of the diode characteristics was confirmed for several hundred times. A characteristic of this molecule-based diode is that the memory of the distribution of charged frozen carriers can be erased when the device is warmed up to ambient temperature. If V_S and V_D were inverted to V_S = 20, V_D = 0 V, and V_G = 0 V, a PN junction was constructed instead (Fig. 6g). In this case, the detected current was only derived from the positive voltage applied (Fig. 7b), again showing that the rectifying function of the molecular diode is erasable and rewritable.

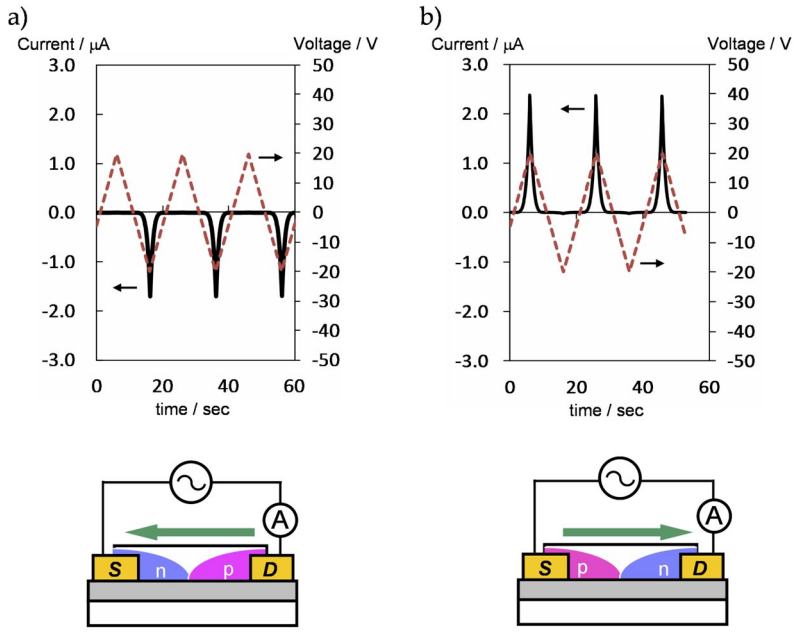

Fig. 7 (a, top) Rectifying characteristics of a molecular diode based on TCT_4Q constructed by application of V_S = 40 V, V_D = 0 V, and V_G = 20 V at 100 K. Dashed lines represent input voltage of V_{p-p} = 40 V, V_G = 0 V, and f = 50 mHz. Thick lines represent the output current under forward bias with $V_S > V_D$ (a, bottom). Molecular diode with NP junction (from left to right) transformed from ambipolar FET: AC is supplied by an AC supplier and the rectified current was recorded by an ammeter. (b, top) Thick lines represents output current under forward bias with $V_S > V_D$ (b, bottom). Molecule-based diode with PN junction (from left to right).

SUMMARY

After the typical ambipolar FET device was constructed using TCT_4Q, it was trained to serve as a molecule-based diode under a set of voltages (V_S, V_D, and V_G). The ambipolar molecule, TCT_4Q, can play various roles in the FET under different external conditions. It is converted to either a negative or positive "mobile" carrier depending on the gate voltage of the FET, providing current through the charge-relay mechanism. Moreover, mobile carriers are easily trapped and the negative or positive "trapped carriers" are converted to the stabilized anion or cation radicals, respectively, owing to the high stability of charged species associated with favorable geometrical changes and stabilization from surrounding molecules. Since the "trapped carriers" become frozen at lower temperature even after removal of the gate voltage, they serve as a floating gate, forming nonvolatile memories or, in other words, a gradient distribution of charged carriers corresponding to the PN or NP junction. This gradient distribution of carriers disappears after warming the device to ambient temperature. The opposite distribution can also be constructed by switching the source and drain voltages, demonstrating that the rectifying function is erasable and rewritable. Such a function makes a sharp contrast to the silicon-based devices, which are precisely designed and operate accurately. The function of the FET device described herein can be changed by external stimuli even after being fabricated. Such a device can be referred to as an "epigenetic" device and represents a unique direction for molecular device development that cannot be fulfilled by conventional silicon-based devices [22].

ACKNOWLEDGMENTS

The authors acknowledge Dr. H. Satoh in Rigaku for his skillful help for X-ray crystallographic analysis. They also thank Prof. T. Toyota for helpful discussion on the mechanism of the diode operation and Mr. I. Mori for his technical support.

REFERENCES

1. J. H. Perlstein. *Angew. Chem. Int., Ed. Engl.* **16**, 519 (1977).
2. R. E. Long, R. A. Sparks, K. N. Trueblood. *Acta Crystallogr.* **18**, 932 (1965).
3. A. Hoekstra, T. Spoelder, A. Vos. *Acta Crystallogr. B* **28**, 14 (1972).
4. C. Simão, M. Mas-Torrent, N. Crivillers, V. Lloveras, J. M. Artés, P. Gorostiza, J. Veciana, C. Rovira. *Nat. Chem.* **3**, 359 (2011) and refs. therein.
5. C. Rost, S. Karg, W. Riess, M. A. Loi, M. Murgia, M. Muccini. *Appl. Phys. Lett*. **85**, 1613 (2004).
6. L. Bürgi, M. Turbiez, R. Pfeiffer, F. Bienewald, H. J. Kirner, C. Winnewisser. *Adv. Mater.* **20**, 2217 (2008).
7. A. Dodabalapur, H. E. Katz, L. Torsi, R. C. Haddon. *Science* **269**, 1560 (1995).
8. T. Yasuda, T. Goto, K. Fujita, T. Tsutsui. *Appl. Phys. Lett.* **85**, 2098 (2004).
9. R. J. Chesterfield, C. R. Newman, T. M. Pappenfus, P. C. Ewbank, M. H. Haukaas, K. R. Mann, L. L. Miller, C. D. Frisbie. *Adv. Mater.* **15**, 1278 (2003).
10. T. D. Anthopoulos, D. M. de Leeuw, E. Cantatore, S. Setayesh, E. J. Meijer. *Appl. Phys. Lett.* **85**, 4205 (2004).
11. M. L. Tang, A. D. Reichardt, N. Miyaki, R. M. Stolenberg, Z. Bao. *J. Am. Chem. Soc.* **130**, 6064 (2008).
12. M. H. Yoon, S. A. DiBenedetto, A. Facchetti, T. J. Marks. *J. Am. Chem. Soc.* **127**, 1348 (2005).
13. H. Higuchi, T. Nakayama, H. Koyama, J. Ojima, T. Wada, H. Sasabe. *Bull. Chem. Soc. Jpn.* **68**, 2363 (1995).
14. J. Casado, L. L. Miller, K. R. Mann, T. M. Pappenfus, H. Higuchi, E. Ortí, B. Milián, R. Pou-Amérigo, V. Hernández, J. T. López Navarrete. *J. Am. Chem. Soc.* **124**, 12380 (2002).
15. J. F. Mooney, A. J. Hunt, J. R. Mcintosh, C. A. Liberko, D. M. Walba, C. T. Rogers. *Proc. Natl. Acad. Sci. USA* **93**, 12287 (1996).
16. D. T. Cromer, J. T. Waber. *International Tables for X-ray Crystallography,* Vol. IV, Table 2.2A, The Kynoch Press, Birmingham (1974).
17. J. A. Ibers, W. C. Hamilton. *Acta Crystallogr.* **17**, 781 (1964).
18. D. C. Creagh, W. J. McAuley. In *International Tables for X-ray Crystallography*, Vol. C, A. J. C. Wilson (Ed.), pp. 219–222, Kluwer Academic, Boston (1992).
19. D. C. Creagh, J. H. Hubbell. In *International Tables for X-ray Crystallography,* Vol. C, A. J. C. Wilson (Ed.), pp. 200–206, Kluwer Academic, Boston (1992).
20. D. E. Janzen, M. W. Burand, P. C. Ewbank, T. M. Pappenfus, H. Higuchi, D. A. da S. Filho, V. G. Young, J. Brédas, K. R. Mann. *J. Am. Chem. Soc.* **126**, 15295 (2004).
21. D. Kawakami, Y. Yasutake, H. Nishizawa, Y. Majima. *Jpn. J. Appl. Phys.* **45**, L1127 (2006).
22. T. Sugawara, M. M. Matsushita. *J. Mater. Chem.* **19**, 1738 (2009).

